# Surface potential response from GaP nanowires synthesized with mixed crystal phases

# Surface potential response from GaP nanowires synthesized with mixed crystal phases

**B Kyeyune[1,2], E Soboleva[1], P Geydt[3], V Khayrudinov[4], P Alekseev[5], H Lipsanen[4] and E Lähderanta[1]**

[1] Department of Physics, LUT University, 53850-Lappeenranta, Finland.
[2] Universität Osnabrück, Barbarastraße 7, 49076 Osnabrück, Germany.
[3] Novosibirsk State University, Pirogova 2, Novosibirsk, 630090, Russia.
[4] Department of Electronics and Nanoengineering, Micronova, Aalto University, 02150-Espoo, Finland.
[5] Laboratory of Surface Optics, Ioffe Institute, 194021-St. Petersburg, Russia.

E-mail: bob@aims.ac.tz

**Abstract.** In this work, we investigate variations of surface potentials along a single gallium phosphide (GaP) nanowire (NW) synthesized with a mixed crystal phase along the growth direction. GaP NWs synthesized with both wurtzite (WZ) and zincblende (ZB) phases were studied. The measurements were performed on a standard Atomic Force Microscopy (AFM) set-up equipped with Kelvin Probe Force Microscopy (KPFM) module in PeakForce Tapping Mode. KPFM Measurements from two structures were analyzed. Variations of surface potentials were observed in a single GaP NW with WZ/ZB segments. An average difference in surface potential was 55±11 mV. This is explained by different crystal structures along the NW. The work expands the understanding of crystal structure-dependent electrical transport properties of GaP NWs.

**Keywords:** Atomic Force Microscopy (AFM), Nanowires (NWs), Kelvin Probe Force Microscopy (KPFM), Wurzite (WZ), Zincblende (ZB), Gallium phosphide (GaP)

## 1. Introduction

Semiconducting nanowire (NW) research has attracted the attention of nanoscience and nanotechnology community due to their fascinating features such as high aspect ratio, high surface area, quantum confinement and the ability to control their crystal structure during growth. In this work, we investigate gallium phosphide (GaP) NWs to broaden the understanding of their surface properties. The study is motivated with the diverse anticipated applications that GaP NWs hold for the NW-based technologies. GaP NWs with a wide direct bandgap is said to be a good candidate for efficient light emitting diodes (LEDs) [1], Effective photoelectrochemical production of hydrogen from water, on p-type WZ GaP NW photocathode, which offers a potential clean and sustainable fuel for the future [2]. GaP NWs have been reported as a good candidates for multi-junction solar cells because of its wide band gap[3]. GaP NWs could also find applications in high-temperature environments like space because of the thermal stability at high temperatures [4].

Before NW-based devices are fabricated for specific applications, there is always a fundamental need to understand their properties. Here we try to understand how mixed crystal

phases (ZB/WZ) in a single NW could affect the surface potential of GaP NWs. Various semiconducting NWs have been fabricated with pure WZ, ZB and ZB/WZ structures. This has opened many research questions in trying to understand how these different phases would affect the properties of the NWs and the performance of NW-based devices. A few examples showing the influence of phase variation in NWs are the following. GaP NWs in their pure ZB structures are said to have an indirect bandgap which limits the efficiency of light emitting diodes (LEDs). A study on GaP NWs fabricated with pure ZB crystal structure demonstrated a direct nature of the bandgap [1]. With such a direct bandgap, the efficiency of LEDs could be improved. Another example is the electric and structural differences between WZ InAs NW and ZB InAs NW. Scanning tunnelling spectroscopy at room temperature revealed band gaps of about 350 meV for ZB InAs and about 390 meV for WZ InAs surfaces[5]. Using surface-sensitive electron microscopy, local vacuum level differences between ZB and WZ were mapped [5]. This would be useful when determining quantities like electron affinity and work function of the InAs NWs for the WZ and ZB surfaces. The influence of the crystal structure on Young's modulus of conical InP NWs has been reported [6] and the study reports Young's modulus value of 130±30 GPa for WZ structures and 65± 10 GPa for the mixed ZB/WZ.

These details show that the different crystal structures influence various properties of the semiconductor nanowires. Such information is necessary when fabricating efficient NW-based device in technological development. To extend the knowledge of crystal phase in semiconductor NWs, here we report the surface potential dependence on crystal structure along GaP NWs grown with mixed phases (WZ/ZB). We do this with the help of Kelvin Probe Force Microscopy (KPFM).

## 2. Sample preparation

Three GaP NW samples in Figure 1 were grown to be investigated for surface potential. The samples were grown with the vapor-liquid-solid growth mechanism in a metalorganic vapor phase epitaxy (MOVPE) reactor on a p-Si (111) substrate. Prior to the growth, the substrates were annealed in-situ at 650 °C for 10 minutes under hydrogen flow to desorb surface contaminants. The substrates were first cleaned inside an ultrasonic bath by soaking them in acetone and in isopropanol for 2 minutes each, followed by 2 minutes rinse in deionized water. 40 nm diameter gold (Au) nanoparticles from a colloidal solution (BBI International, UK) were used in all the samples. A poly-l-lysine solution was applied to the substrates for 30, 10 and 10 s for samples 1, 2, and 3, respectively, to enhance the adhesion of the Au nanoparticles, followed by 30, 10 and 10 s deposition of Au nanoparticles, respectively.

For growth of the GaP NWs, the precursors were trimethylgallium (TMGa) as the group III and tertiarybutylposphine (TBP) as the group V sources. Hydrogen (H) was used as a carrier gas. For sample 1) Figure 1, growth was initiated by simultaneously switching on TMGa and TBP sources for 240 s at a fixed growth temperature of 450 °C. The nominal V/III ratio during the growth was $\sim$ 514, and the TMGa and TBP flow rates were 5.36 $\mu$mol/min and 2750 $\mu$mol/min, respectively. The growth of sample 2 in Figure 1 was initiated by switching on the TMGa and TBP sources simultaneously for 30 s at a fixed growth temperature of 500 °C. The nominal V/III ratio during the growth was approximately $\sim$ 26, and the TMGa and TBP flow rates were 21.42$\mu$mol/min and 550 $\mu$mol/min, respectively. Sample 3 in Figure 1 growth step was started by switching on the TMGa and TBP sources simultaneously for 30 s at a fixed growth temperature of 550 °C. The nominal V/III ratio during the growth was $\sim$100, and the TMGa and TBP flows were 5.36 $\mu$mol/min and 550 $\mu$mol/min, respectively. In all cases, only the TBP flow was kept on after the growth as the reactor was cooled down to 250 °C. NWs in Figure 1 1), were synthesized with length ranging between 3-4 $\mu$m. The NWs were non-tapered. NWs in Figure 1 1) were synthesized with length $\sim$ 5$\mu$m and NWs appeared tapered between 40-70 nm in diameter with many warm like structures. NWs in Figure 1 3) in

showed tapering at 50-140 nm and the structures appeared short with length $\sim 1$ $\mu$m. Figure 1. A Photoluminescence (PL) spectroscopy was performed on the three samples and comparison

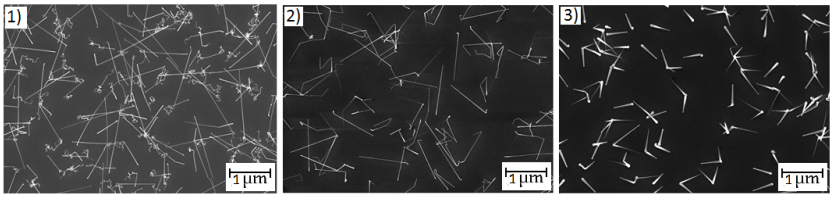


**Figure 1.** Micrograph images of the GaP NW samples 1, 2, and 3 on p-silicon substrate taken by Scanning Electron Microscope (SEM).

on which sample was most suitable for surface potential investigation was made. All samples 1, 2 and 3 were found to have signatures of a mixed phase (WZ/ZB segments). From the PL spectra in Figure 2), the WZ/ZB mixing can be associated to the broad peaks. In this work,

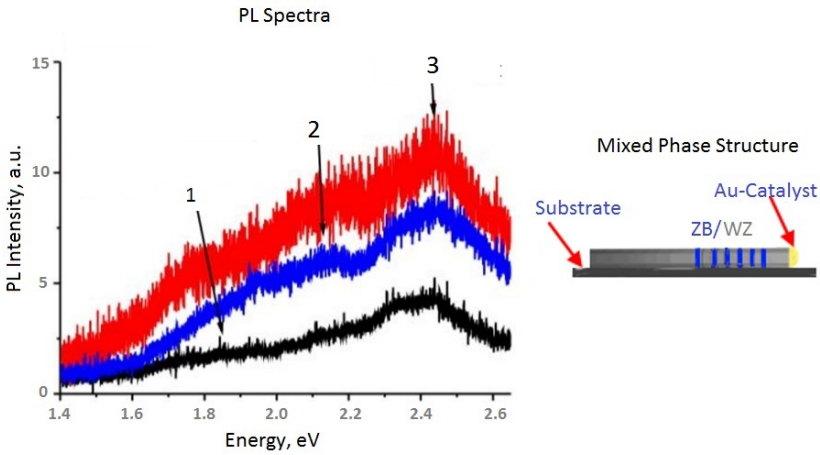


**Figure 2.** A PL spectra for the GaP NW samples 1,2, 3 on the Left and schematic of mixed phase NW with ZB (blue) and WZ (grey) segments on the Right.

we considered the non-tapered GaP NWs grown with WZ/ZB segments to be investigated for surface potentials along a single NW. The structures on sample 2 were considered for surface potential investigation because were long and well spaced for scanning of individual NWs.

Surface potential measurements require that the sample is electrically connected to the sample puck (circular steel disk on which the sample is fixed). GaP NWs on p-Si (111) substrate was attached to a sample puck with conductive silver paste. The level of the paste was uniformly spread on the puck, otherwise it might cause a tilt in the sample which can be seen in the experimental data. The other concern is that the amount of paste should not be too much at the edge of the sample not to touch the cantilever. In a situation where the silver paste is high to contact the cantilever, the circuit will be completed before the tip touches the sample since the dried paste is hard and conductive.

## 3. Experimental Part

Studies to investigate the surface potentials along a single GaP NW with different crystal phase segments were conducted on a Bruker multimode 8 AFM station in ambient conditions. The equipment utilizes PeakForce$^{TM}$ Tapping mode that records force curves at every scanning point, with a periodic modulation of the conductive tip-sample distance. For good potential contrast, we used sharp PFQNE-AL probes (Bruker) with resonance frequency $f_0 \sim 300$ kHz, spring constant $k \sim 0.8$ N/m, a tip radius of 5-15 nm, and tip height $\sim 10$ $\mu$m. The probe was made of silicon tip on a silicon nitride cantilever. PeakForce KPFM is a dual pass mode that serves to minimize crosstalk where in the first pass the sample was scanned and the height data collected. In the second pass (Lift Mode), the NWs were scanned at a lift height of 50 nm to obtain the electrical potential map. To locate lying isolated single GaP NWs on the substrate a survey scan was performed first by disabling the Lift Mode on a scan size of 10 $\mu$m. By zooming in on the desired structures, we enabled the Lift Mode and obtain surface potential maps. Measurements were carried out in a dark room, and the illumination intensity was reduced to as low as 5 % from the camera light controller to minimize the thermal effects.

## 4. Results and Discussions

Figures 3 and 4 show potential profiles along the GaP NW structures with the respective potential maps in the top right corner. The potential maps were taken from sample 2 lying on p-Si substrate. The absolute differences in the surface potential values were taken from different regions along the analysed structures. The observed differences are also significant in contrast as shown in Figures 3 and 4, indicated by different regions brighter less dark regions to higher surface potential regions. To confirm the variations in surface potential, Nanoscope Analysis 1.80 was utilized to perform rectangular box section with equal width of 178 nm on the individual structures for the different regions. The box-sections allowed to decrease the noise level by summarizing the data from few line profiles. The potential profiles were plotted from the extracted raw data with help of MATLAB. For the different regions, as demarcated, the average surface potentials were obtained. The variations in the average surface potentials along the structures were calculated between different regions.

With comparison to the contrast from the potential map shown in Figure 3 b) on the Right NW structure, the potential profile 3 a) showed different distinctive contrasts in different regions A, B, C, and D. The quantitative difference between the average surface potentials in the respective regions are depicted in the Table 1.

**Table 1.** Surface potential differences between different regions along a single NW structure for structure in Figure 3 and Figure 4 .

| Structure | A-B (mV) | A-D (mV) | B-C (mV) | C-D (mV) |
|---|---|---|---|---|
| Figure 3 | 62±26 | 63±22 | 42±22 | 44±17 |
| Figure 4 | 65±37 | - | - | - |

Figure 4 b), is a potential map with varying contrast along the NW in two regions A and B. The potential profile 4 a) indicates the absolute surface potential difference $\sim 65$ mV between the two distinctive regions A and B with varying contrast in the potential. The variation of surface potential can be explained by the crystal structure. The average of surface potential difference in Table 1 is 55 mV±11 mV, where the ±11 mV is the standard error of the mean. We associate these variations to the fact that the NWs were grown with mixed crystal (ZB/WZ) phases which imply different atomic arrangements along the NW surfaces. The difference in the

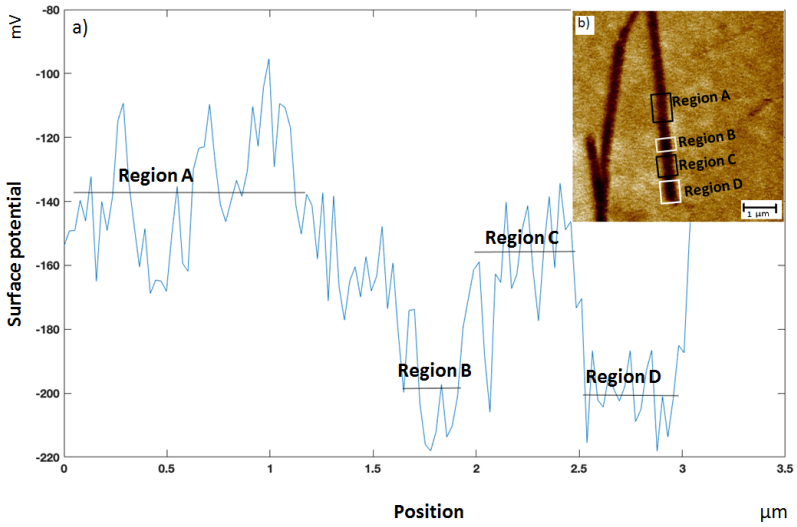


**Figure 3.** a) Potential profile for the labelled structure in potential map b). The horizontal lines on the potential profile represent the average surface potentials in the respective regions as labelled in b). The boxes drawn on the structure in b) demarcate the approximate regions along the NW from which the averages were calculated.

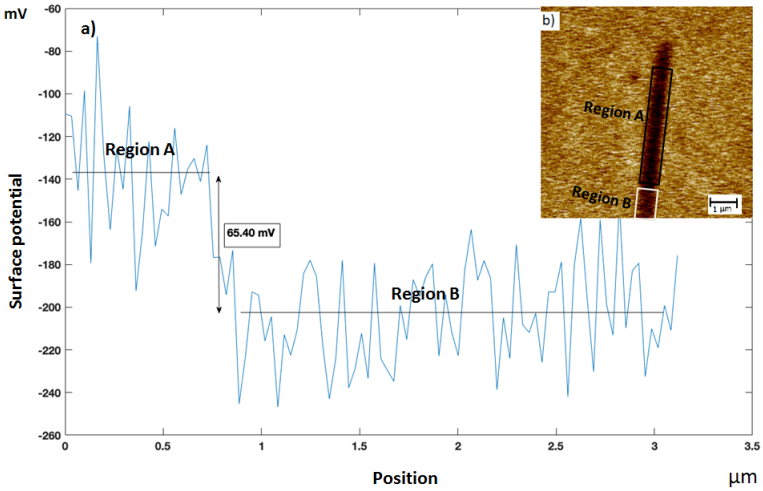


**Figure 4.** a) Potential profile for the labelled structure in potential map b). The horizontal lines on the profile represent the average surface potentials in the respective regions as labelled in b). The boxes drawn on the structure in b) demarcate the approximate regions along the NW from which the averages were calculated.

arrangement patterns of atoms on the surface seems to have significant influence on the surface potential of the GaP NWs.

## 5. Conclusion

We have presented a reproducible surface potential analysis on GaP NW having WZ/ZB crystal phases. A single GaP NW with mixed crystal phases along the growth direction was found to have different surface potential values along the surface. The differences in the surface potential values are explained by the difference in crystal structures along the nanowire. Different crystal structures imply a different atomic arrangement. It is this difference in the arrangement of atoms in the WZ and ZB structures that result in the difference in surface potential along the NW. An average CPD difference of 55 $\pm$11 mV was obtained, with the lowest possible noticeable difference of 42 $\pm$21 mV . We can convince ourselves that GaP NWs with mixed crystal phases will have different surface potential values along the surface. The question of concern remains on which structure posses which surface potential values. Such information would be important for fabrication of NW-based devices. This can be achieved with the help of different measurements techniques like scanning tunneling electron microscopy (STEM) alongside KPFM. Furthermore, since the KPFM measurements were conducted in ambient conditions, this certainly somewhat had some effect on our measurements due to surface contamination[7]. We therefore recommend that measurements would have been preferably performed in UHV.

## Acknowledgments

The research leading to these results has received funding from the EDUFI Fellowship/TM-18-10918. Authors acknowledge the provision of facilities and technical support by Aalto University at Micronova Nanofabrication Centre. V. Khayrudinov acknowledges the support of Aalto University Doctoral School, Walter Ahlström Foundation and Nokia Foundation. P.Geydt thanks CKP VTAN of NSU.

## References

[1] Assali S et al 2013 Direct band gap wurtzite gallium phosphide nanowires *Nano letters* **13** 1559-63.
[2] Standing A, Assali S, Gao L, Verheijen M A, Van Dam D, Cui Y, Notten P H, Haverkort J E and Bakkers E P 2015 Efficient water reduction with gallium phosphide nanowires *Nature communications* **6** 7824.
[3] Lu X, Huang S, Diaz M B, Kotulak N, Hao R, Opila R and Barnett A 2012 Wide band gap gallium phosphide solar cells *IEEE Journal of Photovoltaics* **2** 214-20.
[4] Bittner Z S, Forbes D V, Nesnidal M and Hubbard S M 2011 June Gallium phosphide solar cells with indium gallium phosphide quantum wells for high temperature applications *In 2011 37th IEEE Photovoltaic Specialists Conference* 001959-64
[5] Hjort M et al 2014 Electronic and structural differences between wurtzite and zinc blende InAs nanowire surfaces: experiment and theory *ACS nano* **8** 12346-55.
[6] Dunaevskiy M, Geydt P, Lähderanta E, Alekseev P, Haggren T, Kakko J P, Jiang H and Lipsanen H, 2017 Young's modulus of wurtzite and zinc blende InP nanowires. *Nano letters* **17** 3441-46.
[7] Kahn A, 2016 Fermi level, work function and vacuum level *Materials Horizons* **3** 7-10.